

Journal of Fire Sciences

<http://jfs.sagepub.com>

On the Temperature Measurement Bias and Time Response of an Aspirated Thermocouple in Fire Environment

Sung Chan Kim and Anthony Hamins
Journal of Fire Sciences 2008; 26; 509
DOI: 10.1177/0734904108093516

The online version of this article can be found at:
<http://jfs.sagepub.com/cgi/content/abstract/26/6/509>

Published by:



<http://www.sagepublications.com>

Additional services and information for *Journal of Fire Sciences* can be found at:

Email Alerts: <http://jfs.sagepub.com/cgi/alerts>

Subscriptions: <http://jfs.sagepub.com/subscriptions>

Reprints: <http://www.sagepub.com/journalsReprints.nav>

Permissions: <http://www.sagepub.co.uk/journalsPermissions.nav>

Citations <http://jfs.sagepub.com/cgi/content/refs/26/6/509>

On the Temperature Measurement Bias and Time Response of an Aspirated Thermocouple in Fire Environment

SUNG CHAN KIM*

*School of Fire and Disaster Prevention, Kyungil University
Kyungbuk, 712-701, South Korea*

ANTHONY HAMINS

*Building and Fire Research Laboratory, National Institute of Standards
and Technology, Maryland, 20899, USA*

(Received January 19, 2008)

ABSTRACT: To examine the uncertainty of thermocouple temperature measurements, the present study uses numerical simulations and analytical solutions to investigate the heat transfer processes associated with double shield aspirated thermocouple. This study is divided into two parts. First, 3D CFD calculations for real geometries are performed to understand the flow characteristics of double shielded aspirated thermocouples. Based on iso-thermal flow calculations for real geometry, conjugate heat transfer calculations for a 3D simplified geometry are performed to investigate the thermocouple radiative exchange errors that may be important in a fire environment. The results of the 3D heat transfer calculation are compared with algebraic solutions from a previously developed simple energy balance model and the algebraic model shows acceptable results compared to the 3D CFD model, despite its many assumptions and idealizations. A parametric study was conducted to quantify the thermocouple errors for various gas temperature and

*Author to whom correspondence should be addressed.
E-mail: sungkim@kiu.ac.kr, sungkim.phd@gmail.com
Figures 1–3 appear in color online: <http://jfs.sagepub.com>

JOURNAL OF FIRE SCIENCES, VOL. 26 – November 2008

509

0734-9041/08/06 0509–21 \$10.00/0 DOI: 10.1177/0734904108093516
© SAGE Publications 2008
Los Angeles, London, New Delhi and Singapore

surrounding conditions. In this manner, the present study improves our understanding of the uncertainty of thermocouple temperature measurements.

KEY WORDS: temperature measurement, aspirated thermocouple, fire test, CFD.

INTRODUCTION

ACCURATE MEASUREMENT OF the thermal field is one of the most basic ways to characterize a fire environment. Among the various techniques that can be used to measure the local temperature, bare bead thermocouples with a welded junction are probably the most common, and possibly the easiest to implement. Bare bead thermocouples have been widely used in numerous types of applications for many reasons, including their low cost, convenience, wide temperature range, suitability for large-scale tests, robustness, and so on. In this sense, bare bead thermocouples are an indispensable part of fire research. On the other hand, the uncertainty associated with these measurements may be quite large, depending on the exact application or scenario and the measured temperature may be quite different from the actual gas temperature.

When a bare bead thermocouple is directly exposed to a fire environment, measurement error may result for a variety of reasons, such as radiative exchange between the bead junction and the surrounding environment, heat conduction along the thermocouple wire, soot deposition, thermal inertia, and catalytic effects. In order to reduce the measurement error of a bare bead thermocouple due to radiative exchange, the aspirated thermocouples is increasingly used in fire research applications [1–4]. An aspirated thermocouple is a thermocouple which is shielded from the environment by a cylindrical tube. A gas sample from the location of interest is pulled into the aspiration tube, flowing past the thermocouple. Aspirated thermocouples can have a single or double shield configuration. In either case, the measurement error depends on the details of the environmental and operating conditions.

Recently, several studies have investigated the uncertainty of temperature measurement using bare bead and aspirated thermocouples. Newman et al. evaluated the effectiveness of bare bead and single shield aspirated thermocouples using data from a series of laboratory and room fire experiments [5]. The simple steady heat-balance equations for

aspirated thermocouples were utilized to determine the asymptotic value and compared with the measured results. Brohez et al. used two bare bead thermocouples to estimate radiation error in compartment fires, and a simple practical rule was proposed to estimate the gas temperature using thermocouples with different bead diameters [6]. The simple practical rule was validated with experiments and provided a rough estimate of the measurement bias associated with radiative exchange. Blevins and Pitts developed a steady-state algebraic energy balance model to characterize the bias associated with bare bead, single, and double shielded aspirated thermocouple measurements [7,8]. The effect of the aspiration velocity on the measurement uncertainty was investigated as a function of the conditions in a compartment fire. The simplified energy balance model has provided useful information about thermocouple measurement bias, but its accuracy is unclear, due to its many assumptions and approximations. The analytic model does not consider transient effects, local fluid flow, conductive heat transfer, or important details of the geometric configuration.

In practice, the most cumbersome aspect of the use of an aspirated thermocouple, rather than a bare bead thermocouple, is the need for additional equipment, such as a pump to extract the sample gas, a filter system to remove soot, a cooling trap to remove water from the sample, and a flow-rate measurement system. The double shield aspirated thermocouple and the single shield aspirated thermocouple require the same type of additional equipment. The double shield thermocouple is advantageous in the sense that it provides higher accuracy with no additional equipment requirements.

The present study performed a series of CFD calculations to evaluate the measurement bias and response time, focusing on double shielded aspirated thermocouples. A detailed numerical approach is described in this study, which allows estimation of measurement uncertainty, with consideration of realistic boundary conditions. The numerical results are used to verify results from the simple energy balance model. The 3D CFD results are compared with algebraic solutions of a simplified energy balance model. The thermocouple uncertainty is characterized with the indicated thermocouple temperature and surrounding temperature. The transient CFD solution provides information about the time response of the thermocouple measurement and the time required to experimentally reach steady state. The present study gives a better understanding about the uncertainty of the aspirated thermocouples and can contribute to enhance measurement technology in fire research.

NUMERICAL SIMULATION

A double shielded aspirated thermocouple is rather complicated, geometrically and operationally, whereas a bare bead thermocouple is relatively simple. The prototype aspirated thermocouple investigated in this study is double shielded with an end-hole adapted from NACA (National Advisory Committee for Aeronautics) [9]. Figure 1 shows a schematic drawing of the probe with a close-up view of the inner cylinder and additional equipment. The geometrical complexity and aspiration flow causes a complicated flow field inside this thermocouple. CFD is used to understand the detailed flow characteristics for this geometry, and to provide appropriate boundary conditions for a simplified analytic heat transfer model.

A series of 3D CFD calculations have been performed to characterize the thermocouple bias for various conditions, representative of a compartment fire. Ideally, the CFD simulation would consider details of the flow and heat transfer in the actual geometry, including

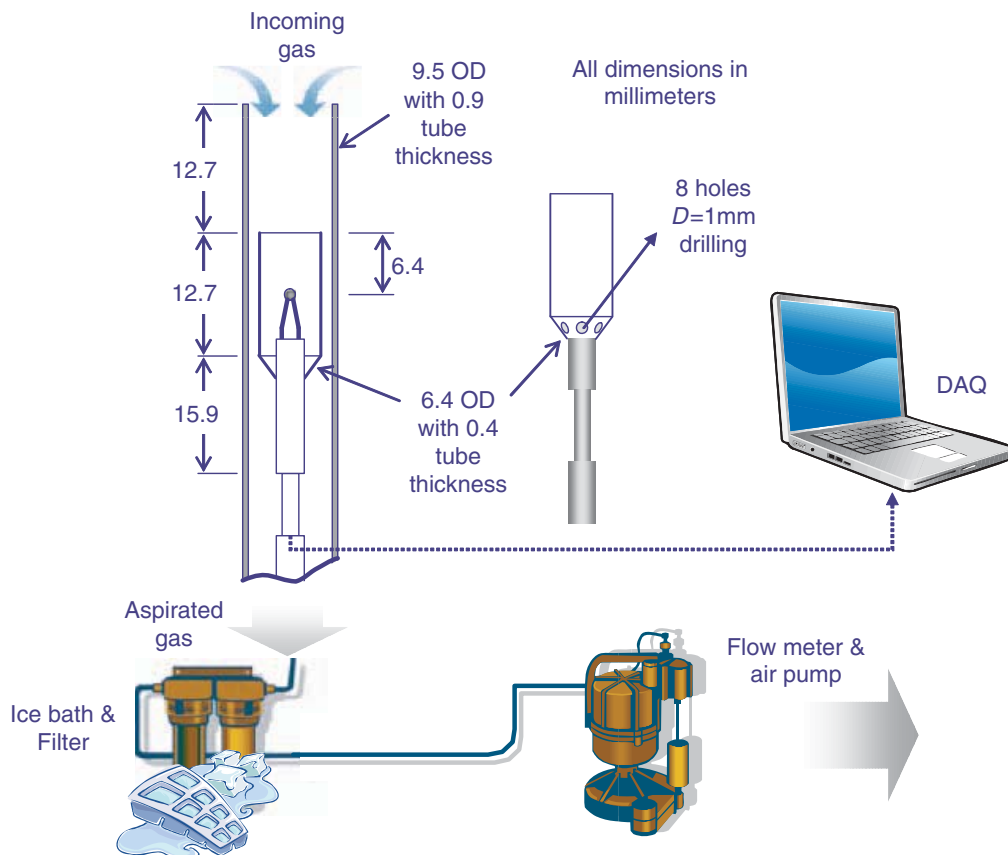


Figure 1. Schematic of the double shield aspirated thermocouple in this study.

turbulence and conjugate heat transfer, but this would require prohibitively expensive computations. For this reason, the CFD calculations were split into two types. The first emphasized detailed calculations of the flow field for a real geometry, while the second involved detailed conjugate heat transfer calculations for a simplified geometry. The first considered the realistic geometry in order to understand details of the flow field associated with the double shield aspirated thermocouple. The second considered a simplified 3D geometry, focusing on details of the heat transfer process and with consideration for conduction, convection, and radiation. Also, algebraic solutions of the previously developed simplified energy balance model [7] were obtained to compare with the 3D CFD results.

CFD Modeling of a Double Shield Aspirated Thermocouple

The flow field is calculated using the commercially available CFD package FLUENT 6.0 to model the flow for given operating conditions [10]. The code is based on the finite volume method on a collocated grid, a nonstaggered grid system is used for the storage of discrete velocities and pressures. The standard $k-\varepsilon$ turbulence model and incompressible the ideal gas assumption were applied to solve the Reynolds stress term and density change, respectively. The governing equation is discretized by the 2nd order upwind scheme in space and the SIMPLE (Semi-Implicit Method for Pressure Linked Equation) algorithm with under-relaxation is used to iteratively solve the momentum equation in their discretized form.

For the 3D flow calculation for the real geometry of a double shield aspirated thermocouple, the computational model includes an inner shield, outer shield, bead thermocouples, and extended domain of the aspirated thermocouples. The computational domain including inside and outside of the aspirated thermocouples is divided into approximately two million cells of tetrahedral type mesh using the ICEM-CFD which is a commercial CAD and grid generation program. Figure 2 shows the computational grid for calculating the flow field in the double shield aspirated thermocouple.

Heat Transfer Modeling for the Simplified Geometry

3D heat transfer calculations including conduction, convection, and radiation were performed to estimate the measurement error for a bare bead and a double shield aspirated thermocouple for idealized simplified geometries. Figure 3 shows a schematic of the idealized double shield

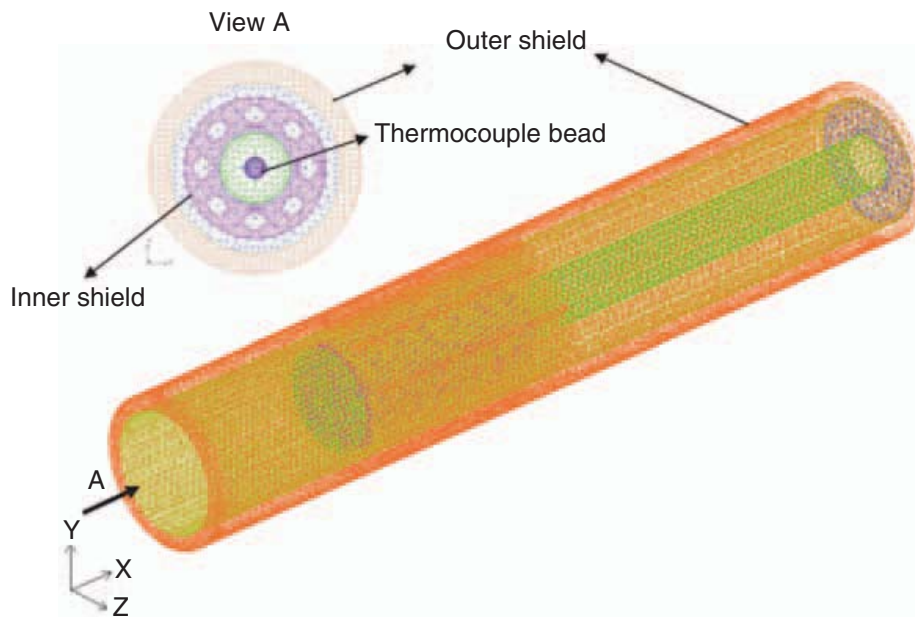


Figure 2. Computational grid for calculating the flow field in the double shield aspirated thermocouple.

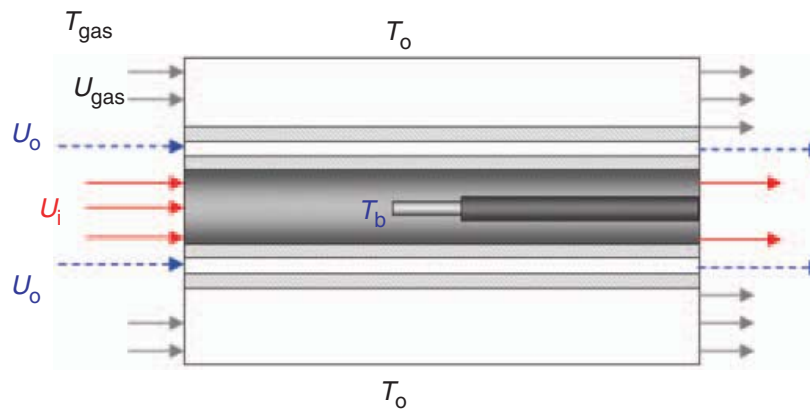


Figure 3. Schematic of the double shield aspirated thermocouple for the simplified heat transfer model.

aspirated thermocouple geometry considered here. The double shield calculation assumed that the flow domain consisted of three flows: a flow outside the outermost shield, an annular flow between the outer and inner shields, and an inner flow within the inner shield. For the bare bead thermocouple calculation, the thermocouple bead was directly exposed to the local environment and the surroundings without shields or aspiration.

Table 1. Properties of solid materials.

Material	Density (kg/m ³)	Specific heat (J/kg K)	Thermal conductivity (W/mK)
Nickel	8.900	460	91.7
Steel	8.030	502	16.3

T_{gas} is the temperature of the incoming gas sample, T_b is the temperature at the thermocouple bead and T_o is the temperature of the surroundings. This study focuses on the difference between T_b and T_{gas} . The incoming flow velocity induced by aspiration was considered. And the material properties of the cylindrical shield and the thermocouple bead were taken as stainless steel and nickel, respectively. This is not an unreasonable approximation as K-type thermocouples are composed of more than 90% nickel. [11]. The properties of solid materials used in this calculation are summarized in Table 1.

Radiative heat transfer was computed using a surface to surface radiation model in which the energy exchange between the two surfaces depends on the view factor, which is a geometric function involving the size, distance, and orientation of surfaces. The surfaces were taken as gray and diffuse, and taken to have a constant Emissivity(ε) equal to 0.8 for comparison with the previous study by Blevins et al. [7]. The gas temperature (T_{gas}) was taken as constant inside and outside of the probe. An external flow velocity (U_{gas}) of 1 m/s and bead diameter of 1 mm was considered for all cases. The representative thermocouples temperature (T_b) was calculated by using a volume weighted average as follows:

$$T_b = \frac{1}{V_b} \int T \cdot dv = \frac{1}{V_b} \sum_{i=1}^N T_{b,i} \cdot dV_i \quad (1)$$

where, V_b is the total volume of the thermocouple bead, $T_{b,i}$ is the individual cell temperature and dV_i represents each cell volume for the solid bead. At the solid – fluid interface, the heat transfer coefficient for laminar flow was computed using Fourier's law:

$$q'' = k_f \left(\frac{\partial T}{\partial n} \right)_{\text{wall}} \quad (2)$$

where q'' is the heat flux to a fluid cell from a wall boundary, k_f is the thermal conductivity of the fluid and n is the local coordinate normal to the wall. For turbulent flows, FLUENT offers two types of functional

approaches to solve heat transfer at walls, which are the standard wall function and a nonequilibrium wall function. The present study uses the standard wall function. The law of the wall for temperature suggested by Launder et al. consists of a linear law for the thermal conduction sub-layer and a logarithmic law for the turbulent region [10,12]. The implicit solver was used to capture the transient characteristics of the heat transfer process between the fluid and the thermocouple bead.

Algebraic solutions of the previously developed simplified energy balance model were obtained by following equations for the double shield aspirated thermocouple [7].

Energy balance for bead

$$h_{b,U_i}(T_{\text{gas}} - T_b) = \varepsilon_b \sigma (T_b^4 - T_{\text{is}}^4) \quad (3)$$

Energy balance for inner shield

$$\begin{aligned} h_{\text{is},U_i}(T_{\text{gas}} - T_{\text{is}}) + h_{\text{is},U_o}(T_{\text{gas}} - T_{\text{is}}) &= -\varepsilon_{\text{is}} \sigma \left(\frac{A_b}{A_{\text{is}}} \right) (T_b^4 - T_{\text{is}}^4) \\ &+ C_{\text{is} \rightarrow \text{os}} \sigma (T_{\text{is}}^4 - T_{\text{os}}^4) \end{aligned} \quad (4)$$

Energy balance for outer shield

$$\begin{aligned} h_{\text{os},U_o}(T_{\text{gas}} - T_{\text{os}}) + h_{\text{os},U_{\text{gas}}}(T_{\text{gas}} - T_{\text{os}}) &= -C_{\text{is} \rightarrow \text{os}} \sigma \left(\frac{A_{\text{is}}}{A_{\text{os}}} \right) (T_{\text{is}}^4 - T_{\text{os}}^4) \\ &+ \varepsilon_{\text{os}} \sigma (T_{\text{os}}^4 - T_o^4) \end{aligned} \quad (5)$$

where, h is the convective heat transfer coefficient, ε is the emissivity, and σ is Stefan–Boltzmann constant. The subscripts of is and os represent the inner and outer shield.

RESULTS

Flow Field of the Realistic Geometry of a Double Shield Aspirated Thermocouple

Figure 4 shows the calculated pressure and velocity field for the double shield aspirated thermocouples with an aspiration flow rate of 24 L/min. The entrance area of the inner shield is larger than its exit area, which is comprised of eight holes (Figure 2). This blockage effect

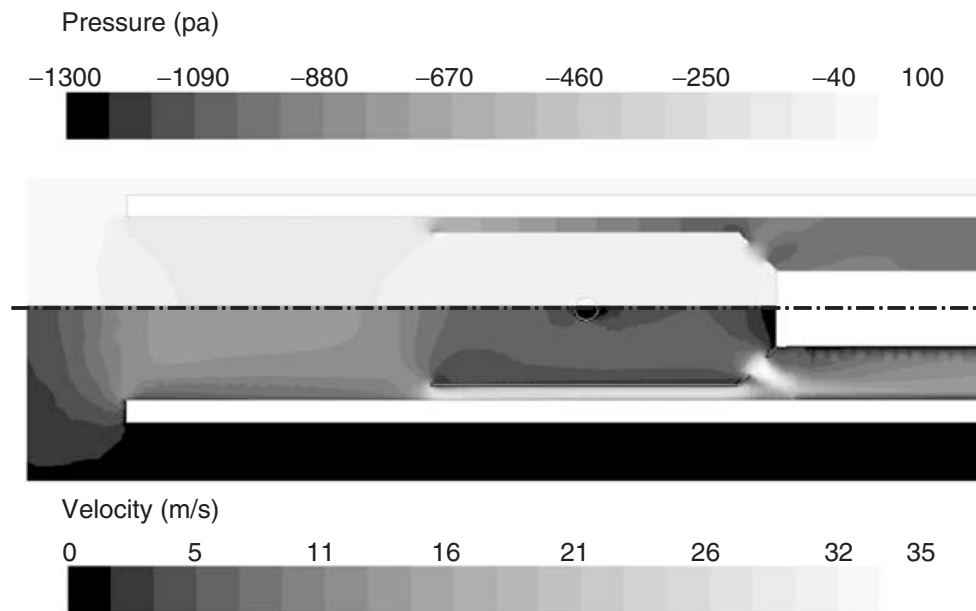


Figure 4. Calculated pressure and velocity fields in the double shield aspirated thermocouple at the gas temperature of 300 K (aspiration flow rate = 24 L/min).

creates a high stagnation pressure at the end of the inner shield, leading to an adverse pressure gradient inside of the inner shield. This high static pressure inside of the inner shield causes the aspirated gas flow to pass through the outer passage with a relatively high velocity. The flow blockage effect in the inner shield lead to a velocity difference between the inner and the outer annular passage, which affects the convective heat transfer in the double shield aspirated thermocouples.

Figure 5 presents the maximum flow velocity of the inner shield ($U_{i,max}$) and the outer annular passage ($U_{o,max}$). The ratio of these velocities is also shown. Here, the maximum velocity ratio (ζ) is defined as:

$$\zeta = \frac{U_{o,max}}{U_{i,max}} \quad (6)$$

Figure 5 shows that the velocity ratio increases as the aspiration flow rate increases and that the maximum velocity in the outer passage is about three times higher than that of the inner shield for nominal operating conditions (24 L/min at STP). This information was used to determine the velocity boundary conditions in the simplified geometry CFD heat transfer calculation and in the analytic energy balance model.

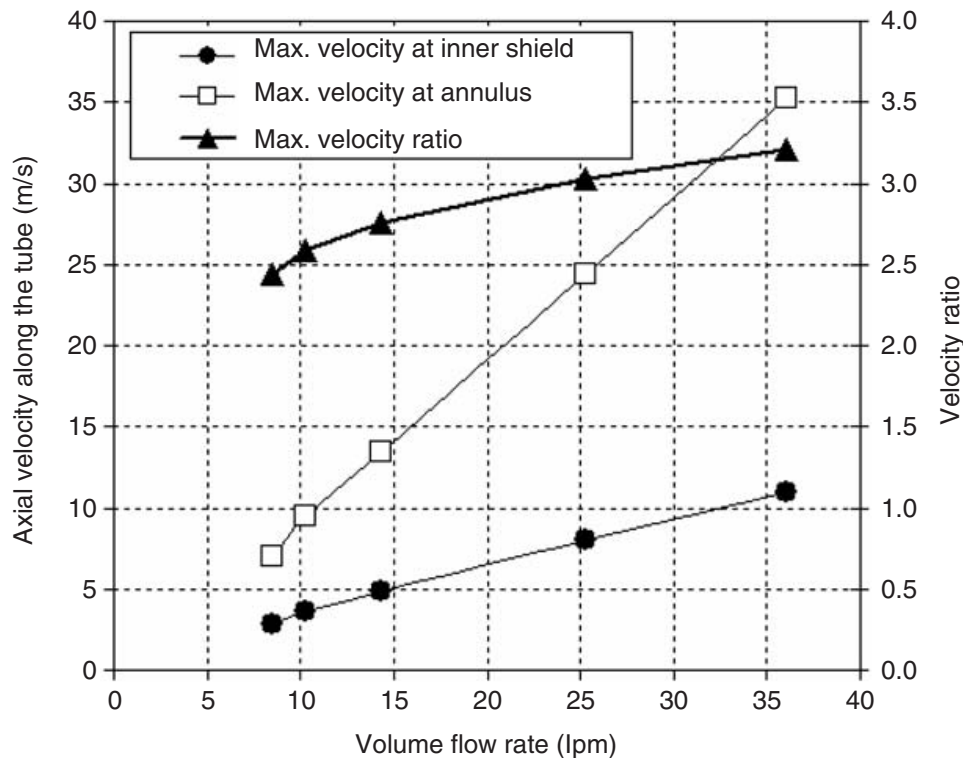


Figure 5. Comparison of the maximum axial velocity for double shielded aspirated thermocouples ($T_g = 300$ K).

Conjugate Heat Transfer Calculation for the Simplified Geometry

Figure 6 compares the predicted temperature of the bare bead thermocouple using the algebraic simple energy balance model with the result from the CFD model considering conjugate heat transfer for an external flow with a velocity of 1 m/s and a gas temperature of 300 K and 900 K. The maximum difference of the predicted thermocouple temperature between the algebraic model and the CFD model was about 50 K for the two gas temperatures considered.

Despite the simplicity of the algebraic model, the results predicted by the algebraic model were in reasonable agreement with the CFD model for the bare bead thermocouple exposed to the surroundings over a broad temperature range. For a 900 K gas temperature, the maximum difference between the CFD model and the algebraic model occurred for a surrounding temperature (T_o) of 300 K. The thermocouple error, that is the difference between the incoming gas temperature and the predicted thermocouple temperature, was about 160 K for the

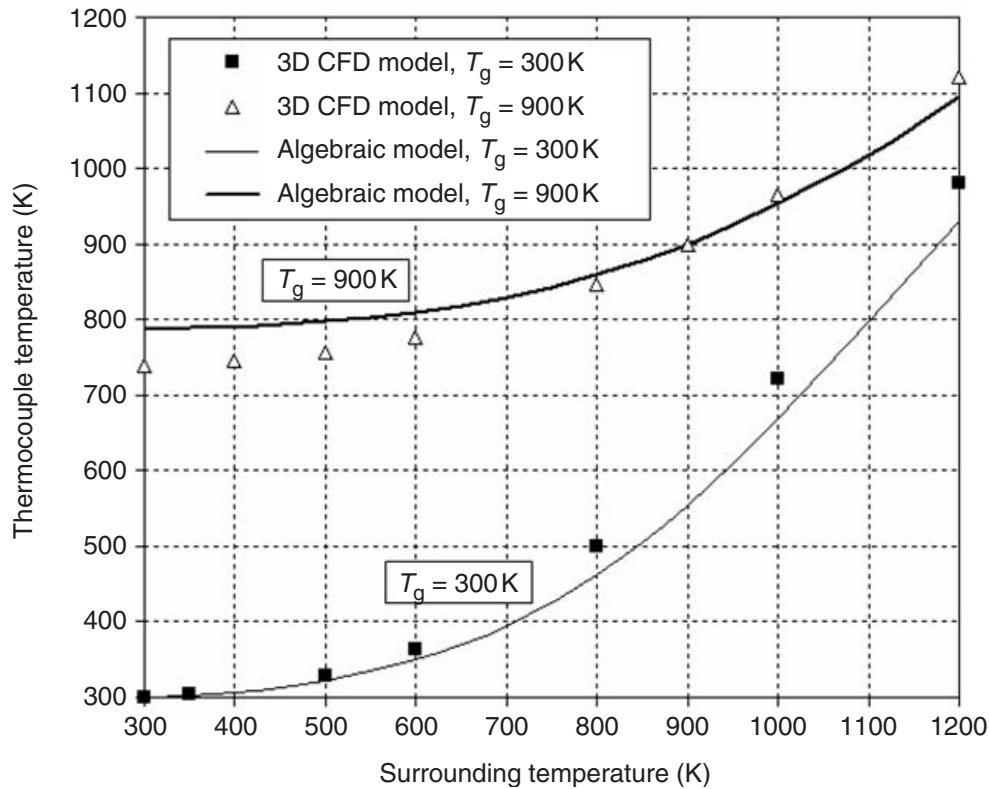


Figure 6. Comparison of the predicted bare bead thermocouple temperature between the algebraic model and the 3D CFD model for an external gas velocity of 1 m/s.

CFD model, which was 50 K higher than that of the algebraic model. But for a 300 K gas temperature, the maximum difference between CFD model and algebraic models occurred for the highest surrounding temperature, and increased with increasing surrounding temperatures. The results show that for a gas temperature of 300 K, the thermocouple error of a bare bead thermocouple exceeds 100 K, when the surrounding temperature was higher than 700 K.

Figure 7 shows the thermocouple temperature of a double shield aspirated thermocouple predicted by the algebraic and CFD models for an aspiration flow rate of 24 L/min. The inlet boundary conditions for the aspirated gas at the inner and outer annular tubes were applied with the velocity calculated using the 3D CFD model with a realistic geometry. For a gas temperature of 600 K, both predictions match within 1% for the overall surrounding temperature. For gas temperature higher than 600 K, the thermocouples error predicted by the algebraic model was less than the CFD model, with the maximum difference between the algebraic model and the CFD model equal to about 50 K.

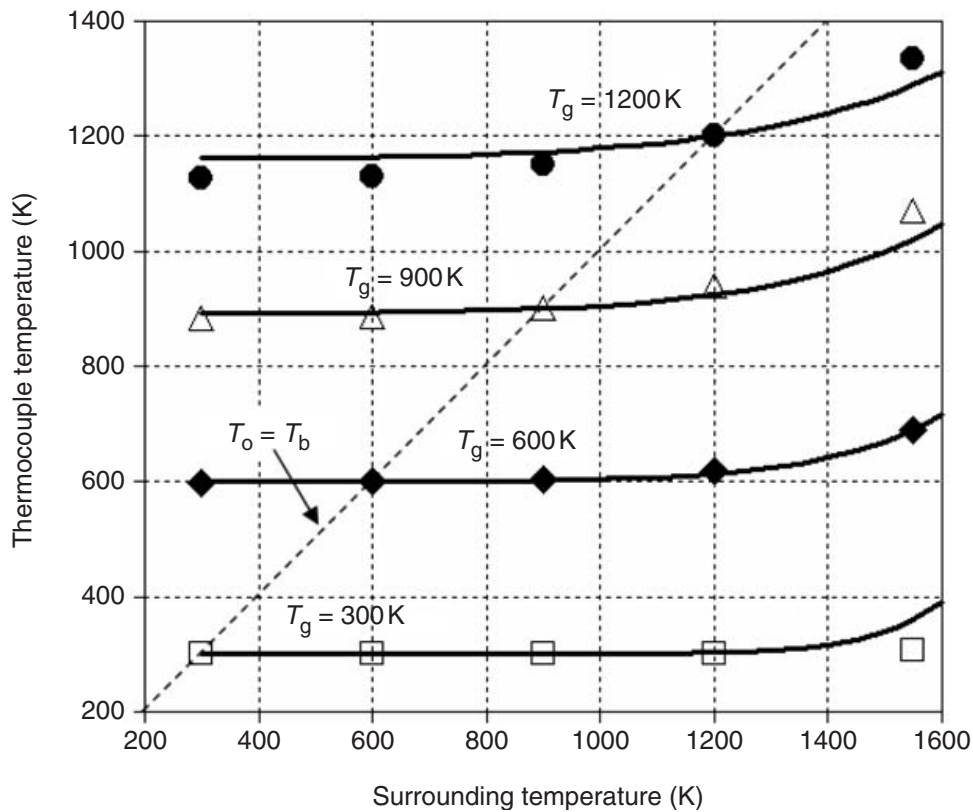


Figure 7. Comparison of the predicted double shield thermocouple temperature between the algebraic model and 3D CFD model for an aspiration flow rate of 24 L/min. (symbols represent the CFD model, lines represent the algebraic model).

But for a gas temperature of 300 K, the thermocouple error of the algebraic model was larger than the CFD model. The thermocouple error increased as the temperature difference between the gas and surrounding increased. The thermocouple error increased for the higher surrounding temperature, while it was approximately constant for a lower surrounding temperature. Considering overall performance, solution of the algebraic model shows acceptable results compared to the 3D CFD model, despite the larger number of assumptions and idealizations. This agreement shows that the algebraic energy balance model is adequate to estimate thermocouple bias for this particular application. Figure 8 depicts the map of the calculated thermocouple error for a double shield aspirated thermocouple as a function of the thermocouple bead (T_b) and surrounding (T_o) temperatures determined using the 3D CFD model. The map shows two regimes of significant error for the thermocouple temperature measurement. The first occurs for relatively low temperature surroundings, in which the gas temperature is systematically under-predicted, notably for higher

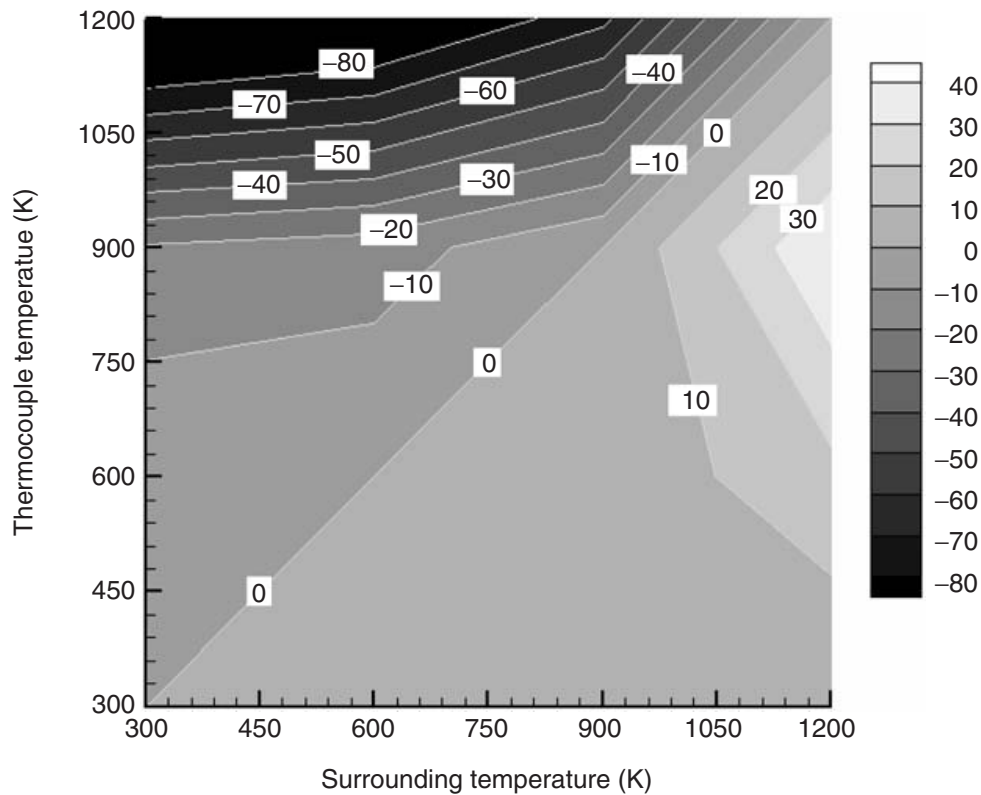


Figure 8. A map of the measurement bias of a double shield aspirated thermocouple as a function of the thermocouple temperature and the surrounding temperature determined using the 3D CFD model.

gas temperatures. The temperature error in this regime varied with the gas temperature, but was as large as -100 K for an indicated thermocouple temperature of 1200 K. The other regime with significant error occurred for high surrounding temperatures, in which the gas temperature was over-predicted.

The maximum error in this regime was as large as 40 K for a high surrounding temperature ($T_o = 1200$ K) and a thermocouple temperature of about 900 K. The results calculated by the algebraic model showed similar trends, but the magnitude of the difference was smaller. As seen in Table 2, the use of the double shield aspirated thermocouple dramatically reduced the thermocouple error as compared to a bare bead thermocouple for a gas temperature of 300 K. The temperature measured using the double shield aspirated thermocouple was close to the true gas temperature regardless of the value to the surrounding temperature (T_o). For a relatively high gas temperature (900 K), the bias of the double shield aspirated thermocouple was relatively large compared to its performance for a gas temperature of 300 K.

Table 2. Calculated thermocouple temperature bias.

T_g (K)	$T_b - T_g$ (K)			
	Bare bead thermocouple		Double shield aspirated thermocouple	
	$T_o = 300$ K	$T_o = 1200$ K	$T_o = 300$ K	$T_o = 1200$ K
300	0	680	0	3
900	-160	220	-10	120

Its performance, however, was still superior to that of the bare bead thermocouple. In summary, the use of a double shield aspirated thermocouple can be expected to reduce measurement error, particularly for lower layer compartment fire environments.

To design the geometrical configuration of a double shield aspirated thermocouple, it is important to examine the optimal velocity ratio of the flow in the inner tube to the flow in the outer annular tube. The present study investigated the effect of the velocity ratio on the thermocouple measurement bias for a given aspiration flow of 24 L/min. Figure 9 shows the temperature bias associated with various velocity ratios for two conditions involving significant differences between the incoming gas temperature T_{gas} and the thermocouple bead temperature T_b . For conditions such that the gas temperature was 1550 K and the surrounding temperature was 300 K, the temperature bias was larger than 190 K, and temperature bias varied about 20 K over a large range of velocity ratios (from 0.2 to 17). The temperature bias was a minimum for a velocity ratio between 2 and 3. For the case of a gas temperature of 900 K and surrounding temperature of 1550 K, the temperature bias was larger than 170 K, with a maximum difference in the temperature bias of about 60 K as the velocity ratio was varied. The temperature bias also exhibited a minimum value for a velocity ratio between 2 and 3. This indicated that the optimal velocity ratio to minimize thermocouple bias was about 3 for a flow of 24 L/min and the geometry of the double shield aspirated thermocouple considered in the present study.

Time Response of the Double Shield Aspirated Thermocouple

The time response of the thermocouple measurements was investigated using CFD modeling. The algebraic model can not provide this type of information, because the transient term in the energy balance equation is not considered. Figure 10 shows the time history of the calculated thermocouple response for a double shield

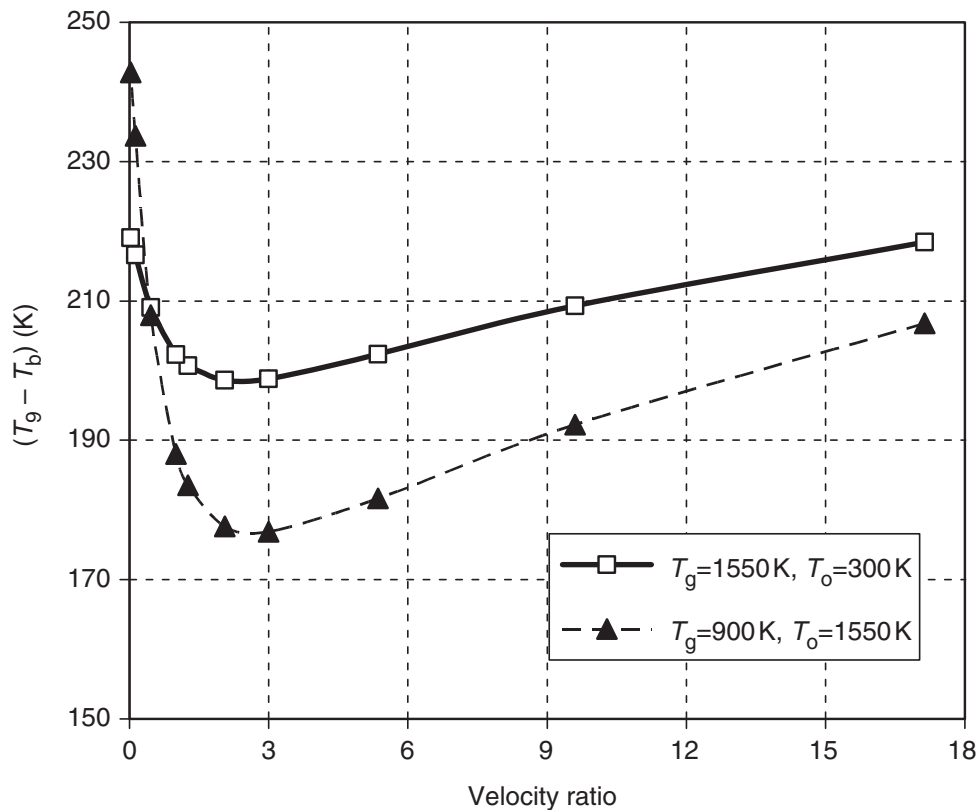


Figure 9. Effect of velocity ratio on the thermocouples effectiveness for the double shield aspirated thermocouple for a given aspiration flow rate of 24 L/min. (T_b is the thermocouple temperature, and T_{gas} is the incoming gas temperature).

aspirated thermocouple. Initially, the gas and thermocouple temperature was assumed to be the same as the surrounding temperature and the aspiration rate was assumed to be 24 L/min. In the calculation, the temperature was specified to rise or fall towards the quasi steady-state temperature over tens of seconds; the exact time depended on the magnitude of the temperature change. For all cases considered in this study, the time to reach a quasi steady-state temperature was less than 50 s, and the thermocouple bias was less than 0.1% after 50 s. In order to characterize the response time for a range of initial and surrounding temperatures, a nondimensional temperature (T^*) is introduced:

$$T^* = \frac{T - T_{SS}}{T_i - T_{SS}} \quad (7)$$

where, T_i the initial temperature and T_{SS} is the quasi-steady state temperature at time equal to 100 s. Figure 11 shows the time history of nondimensionalized temperature of double shield aspirated

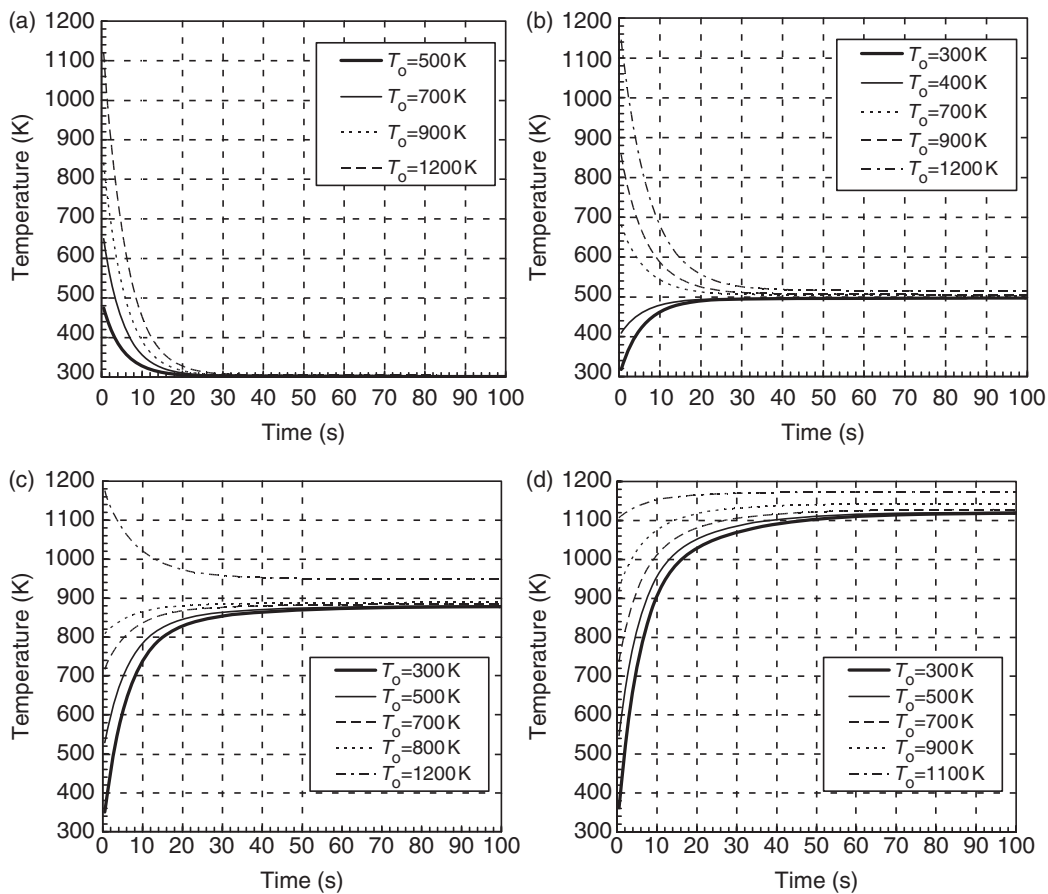


Figure 10. The calculated time history of the temperature of a double shielded aspirated thermocouple for various incoming gas and surrounding temperatures and an aspiration flow of 24 L/min: (a) $T_g = 300$ K; (b) $T_g = 500$ K; (c) $T_g = 900$ K; (d) $T_g = 1200$ K.

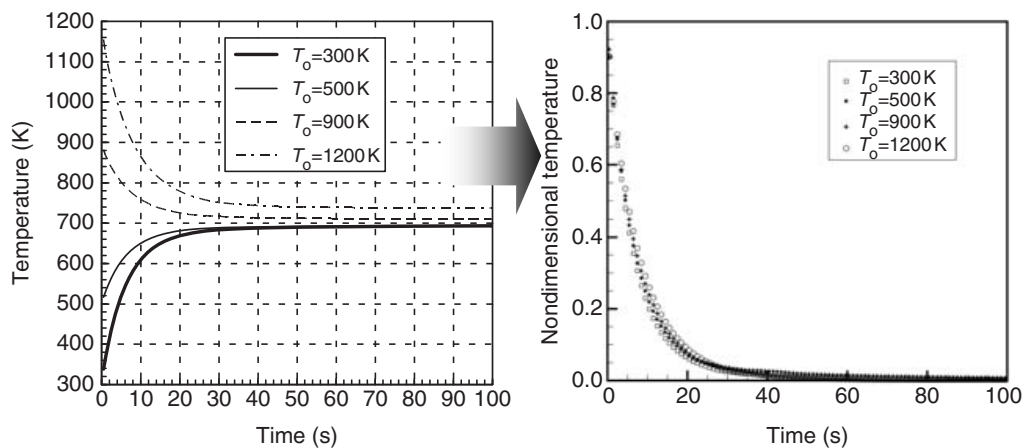


Figure 11. The calculated time history of the temperature and non-dimensionalized temperature of a double shielded aspirated thermocouple for incoming gas of 700 K and an aspiration flow of 24 L/min.

thermocouple for gas temperature of 700 K and an aspiration flow rate of 24 L/min. The time history of nondimensional temperature clearly shows that the time response of thermocouple is well matched with each other for various surrounding temperature and given gas temperature. Figure 12 shows the calculated time history of nondimensional temperature of a double shield aspirated thermocouple for the various combinations of gas temperature and surrounding temperature for an aspiration flow rate of 24 L/min. The error bars represent the standard deviation of thermocouple temperature for different surrounding temperatures at given gas temperature. The calculation shows that the thermocouple responds faster at lower gas temperatures.

In order to quantify the thermocouple time response, a time constant (τ) is introduced that is defined as the time required by a sensor to reach a specified temperature under specific conditions:

$$T^*(t) = T^*(0) \cdot e^{-t/\tau} \quad (8)$$

where $T^*(t)$ is the nondimensional temperature at time and $T^*(0)$ is the nondimensional initial temperature value. When time (t) is equal to τ , then $T^*(t)/T^*(0)$ is 0.368, meaning that the temperature has changed about 63% from its initial temperature value in one unit of the time constant. Three time constants (3τ), which represents about a 95% temperature change from the initial state, is commonly used to characterize the response time for practical systems [13]. As seen in Figure 12, the time constant (τ) varied from about 5 to 11 s, so that

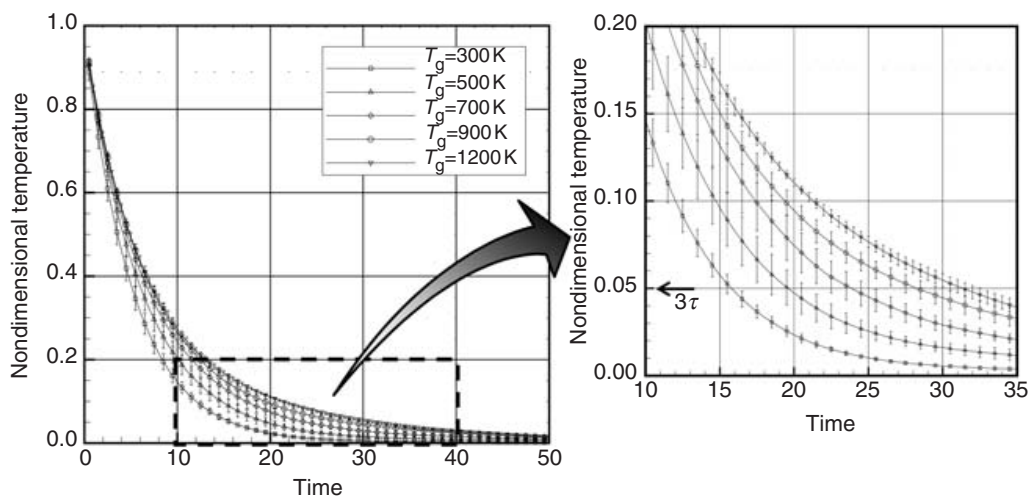


Figure 12. The calculated time history of non-dimensional temperature of a double shielded aspirated thermocouple for an aspiration flow of 24 L/min.

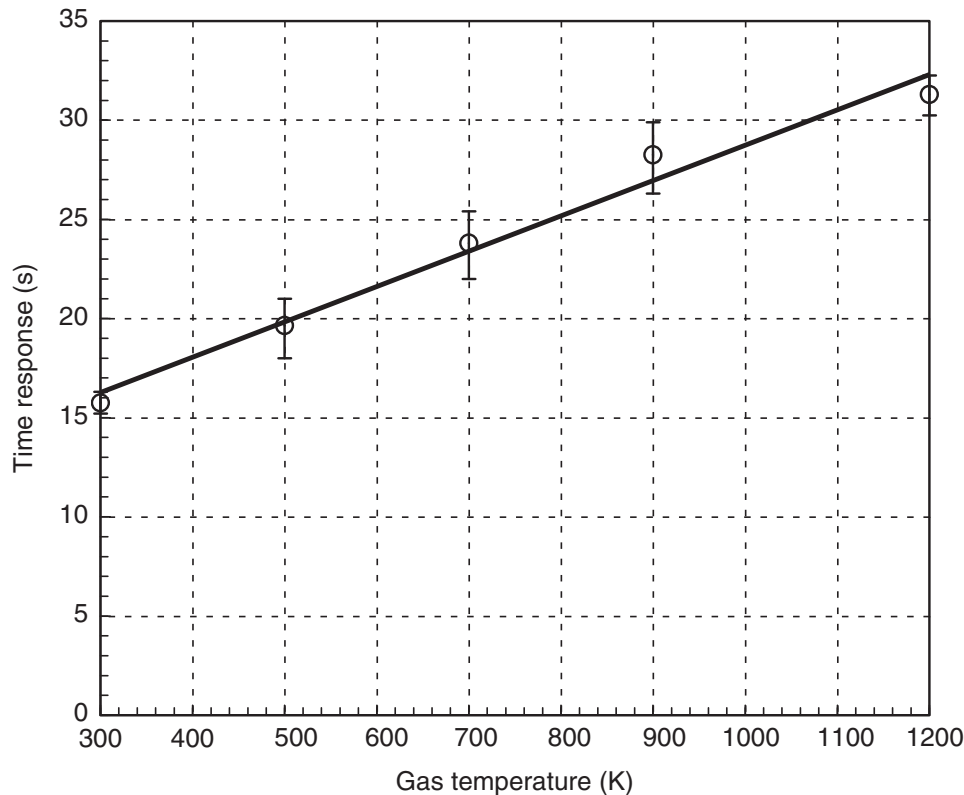


Figure 13. The response time of a double shielded aspirated thermocouple for an aspiration flow of 24 L/min.

the response time ($=3\tau$) varied from 15 to roughly 30 s. Figure 13 shows the time response (3τ) of the double shield aspirated thermocouple as a function of the gas temperature for an aspiration flow rate of 24 L/min. The figure shows that the response time increased with increasing gas temperature and varied from 15 to 30 s, following the trend in gas temperature.

CONCLUSIONS

The present study investigated the flow and heat transfer characteristics of a double shield aspirated thermocouple using an algebraic energy balance model and a 3D CFD model. Despite the application of additional assumptions and idealizations, calculations using the previously developed algebraic energy balance model [7] generally showed good agreement with the results of the 3D CFD model. The algebraic model can be useful, particularly in parametric studies used to evaluate thermocouple measurement error. Consistent with previous findings,

calculations show that use of the double shield aspirated thermocouple can greatly reduce the thermocouple error especially for low gas temperatures. The results, however, can still be biased by hundreds of degrees, depending on the conditions. A map of the thermocouple systematic error for the double shield aspirated thermocouple provides information on the order of magnitude of the measurement error for a given surrounding temperature. The results of the CFD model allow determination of the transient response of the double shield aspirated thermocouple, which is helpful in the interpretation of measurement results and possibly for design of the experiment itself. The present study improves our understanding of the uncertainty of thermocouple temperature measurements and also can contribute to validate fire models and to enhance the reliability of measurement data for standard test methods.

The temperature measurement error under real fire conditions may differ from the results of the present study because the results were calculated for extreme and worst cases such as large temperature difference between the gas and the surroundings, and abrupt change of gas temperature for calculating thermocouple response. The results in the present study should be considered representative of the maximum bias of measured temperature in the compartment fire. The intent of the present study was to provide useful information on measurement bias of thermocouples. Further and more detailed calculations that consider the actual fire conditions along with experimental validation of the measurement bias of thermocouples are still necessary for an accurate estimate of the aspirated temperature measurements.

ACKNOWLEDGMENT

The authors are grateful to Matthew Bundy, Erik Rik Johnsson, and Gwon Hyun Ko for helpful discussions and technical support.

REFERENCES

1. Rutherford, L. (2002). *Pre-Flashover Fire Experiments in Two Adjacent ISO Compartments*, Chapter 2. Experimental, MS Thesis University of Canterbury, New Zealand.
2. Shield, T.J., Silcock, G.W.H., Moghaddam, A.Z., Azhakesan, M.A. and Zhang, J. (1999). A Comparison of Fire Retarded and Non-fire Retarded Wood-based Wall Linings Exposed to Fire in an Enclosure, *Fire and Materials*, **23**(1): 17–25.

3. Hamins, A., Maranghides, A., McGrattan, K.B., Ohlemiller, T.J. and Anleitner, R.L. (2005). Experiments and Modeling of Multiple Workstations Burning in a Compartment, NIST NCSTAR 1-5E, Federal Building and Fire Safety Investigation of the World Trade Center Disaster.
4. Fluent Inc., FLUENT 6.0 User's Guide, 2001.
5. Newman, J.S. and Croce, P.A. (1979). A Simple Aspirated Thermocouple for Use in Fire, *Journal of Fire and Flammability*, **10**(4): 327–336.
6. Brohez, S., Delvosalle, C. and Marlair, G. (2004). A Two-thermocouples Probe for Radiation Corrections of Measured Temperatures in Compartment Fires, *Fire Safety Journal*, **39**(5): 399–411.
7. Blevins, L.G. and Pitts, W.M. (1999). Modeling of Bare and Aspirated Thermocouples in Compartment Fires, *Fire Safety Journal*, **33**(4): 239–259.
8. Blevins, L.G. (1999). Behavior of Bare and Aspirated Thermocouples in Compartment Fires, In: *Proceeding of the 33rd National Heat Transfer Conference*, Albuquerque, New Mexico.
9. Glawe, G.E., Simmons, F.S. and Stickney, T.M. (1953). Radiation and Recovery Corrections and Time Constants of Several Chromel-Alumel Thermocouple Probe in High Temperature, High Velocity Gas Streams, NACA TN3766.
10. Fluent 6.0 user's guide. (2003). Fluent Inc.
11. Burns, G.W. and Scroger, M.G. (1989). *The Calibration of Thermocouples and Thermocouple Materials*, Chapter 2. Principles of Thermoelectric Thermometry, NIST Special Publication 250-35, Gaithersburg, MD.
12. Launder, B.E. and Spalding, D.B. (1974). The Numerical Computation of Turbulent Flows, *Computer Methods in Applied Mechanics and Engineering*, **3**(2): 269–289.
13. Akers, A., Gassman, M. and Smith, R. (2006). *Hydraulic Power System Analysis*, Chapter 5. Linear System Analysis, CRC, Taylor and Francis.

BIOGRAPHIES

Sung Chan Kim

Sung Chan Kim received the B.S (1997) degree in Naval Architecture from Korea Maritime University, and the MS (1999) and PhD (2003) degrees in Mechanical Engineering from Chung-Ang University, Korea. He was a Guest Scientist in Building and Fire Research Laboratory, NIST for two years. His current interests include measurement uncertainty of fire tests, thermal imaging technology for fire fighting, advanced fire detection based on USN (Ubiquitous Sensor Network), and water mist fire suppression system.

Anthony Hamins

Anthony Hamins received a B.S. (1979) in Physics from University of California at Berkeley and a PhD (1985) in Engineering Physics from University of California at San Diego. He has been at NIST since 1989 and is Chief of the Fire Research Division. His research interests include advanced measurement and predictive methods in fire research, the structure and extinction of nonpremixed flame, micro-gravity combustion, validation of fire models, compartment fires, fire suppression in full-scale vehicle and structures, and thermal imaging technology.